Water-Assisted Interconversions and Dissociations of the Acetaldehyde Ion and Its Isomers. An Experimental and Theoretical Study†

Xian Wang, Weixing Sun, and John L. Holmes*

Chemistry Department, University of Ottawa, 10 Marie-Curie, Ottawa, Ontario K1N 6N5, Canada

Received: December 6, 2005; In Final Form: March 7, 2006

The gas-phase reactions of the ion $[CH_3CHO/H_2O]^{+\bullet}$ have been investigated by mass spectrometry. The metastable ion (MI) mass spectrum reveals that this ion−molecule complex decomposes spontaneously by the losses of H_2O, CO, and $^{\bullet}CH_3$. The structures of stable complexes and transition states involved in the potential energy surface (PES) have been studied by the G3//B3-LYP/6-31+G(d) computational method. Hydrogen-bridged water complexes have been found to be the major products of the losses of CO and $^{\bullet}CH_3$. The CO loss produces the $[^{\bullet}CH_3\cdots H_3O^+]$ ion and involves a "backside displacement" mechanism. The products corresponding to $^{\bullet}CH_3$ loss have been assigned by theory to be $[OC\cdots H_3O^+]$ and $[CO\cdots H_3O^+]$, and their 298 K enthalpy values, calculated at the G3 level of theory, are $\Delta_f H[OC\cdots H_3O^+] = 420$ kJ/mol and $\Delta_f H[CO\cdots H_3O^+] = 448$ kJ/mol. The PES describing the interconversions among water-solvated $CH_3CHO^{+\bullet}$, $CH_3COH^{+\bullet}$, and $CH_2CHOH^{+\bullet}$ have been shown to involve proton-transport catalysis (PTC), catalyzed 1,2 H-transfer, and an uncatalyzed H-atom transfer mechanism, respectively.

Introduction

Since the mid-1970s, many authors have reported that ion−molecule and/or ion−neutral complexes can be key intermediates in the reactions of organic ions.[1−5] The interconversions between isomeric ions have been extensively studied, and in many circumstances, the energy barrier separating two isomers exceeds the lowest energy dissociation limit of one of them and thus they cannot freely interconvert. Recent studies[6−10] have been carried out on the catalyzed isomerization of a radical ion that is electrostatically bound to (solvated by) a selected neutral molecule, as for example in proton-transport catalysis (PTC) which involves the reversible H^+ transport between the ion and the neutral moiety:

$$\underset{}{HAB^{+\bullet} + M \rightarrow [HAB^{+\bullet}\cdots M] \rightarrow} \underset{I}{} \underset{}{[AB^{\bullet}\cdots {}^{+}HM] \rightarrow} \underset{II}{} \underset{}{[ABH^{+\bullet}\cdots M] \rightarrow ABH^{+\bullet} + M} \quad (1) \underset{III}{}$$

For the PTC mechanism to operate, a necessary criterion must be met, namely, that the proton affinity (PA) of the catalyst, M, must lie between the PA values for the radical and heteroatom sites in $AB^{\bullet}$, a rule which was established by the calculations of Chalk and Radom.[10] However, proton affinity is not the only criterion for successful catalysis. For example, methanol ions can be catalytically converted into their distonic form by a noble gas[11] (Ar, Kr, Xe), by N_2,[11] and by methanol itself.[12] In the former case, the PA of the neutral gas is lower than that of the $^{\bullet}CH_2OH$ radical at both the C and O sites, and in the latter case, the PA of methanol is higher than that of either site. Self-catalysis by methanol involves a reversible intraionic 1,2 hydrogen atom shift.[12]

We have found that many more than three isomeric structures (as shown in eq 1) of an ion−molecule pair are accessible when an ion is electrostatically attached to a molecule, rather than only a single catalyzed isomerization of the ion by the neutral moiety.[13,14] These stable species lie in separate potential wells and can undergo characteristic dissociations and/or isomerizations between isomeric configurations, and such reactions may involve both catalyzed and uncatalyzed reaction paths. Recent work in our laboratory has used a collision-induced dissociation (CID) method to generate ion−molecule complexes, a routine that allows us to explore much of the chemistry of the accessible stable and metastable isomeric species. These studies provide otherwise inaccessible information relating to simple bimolecular reactions, that is, collision encounters between the ion and the neutral molecule.

The water-assisted isomerization of the methanol ions, $CH_3OH^{+\bullet}/H_2O \rightleftharpoons {}^{\bullet}CH_2OH_2^+/H_2O$, has been investigated in detail.[6,7,15,16] In this system, the PTC mechanism can operate because the PA of the catalyst, H_2O, meets the PA criterion for PTC; that is, it lies between the PA value of the C and O sites of the $^{\bullet}CH_2OH$ radical ($PA[H_2O] = 691$ kJ/mol;[17] $PA[^{\bullet}CH_2OH]$ at O = 695 kJ/mol[17] and at C = 663 kJ/mol[17]). The catalyzed reaction is calculated to proceed with less than half the activation energy of the unimolecular rearrangement of $CH_3OH^{+\bullet}$ to $^{\bullet}CH_2OH_2^+$. Note that the uncatalyzed activation energy (108 kJ/mol) exceeds the dissociation limit (66.2 kJ/mol) for $CH_3OH^{+\bullet} \rightarrow {}^{+}CH_2OH + H^{\bullet}$.[6,7]

Nedev et al.[18] studied the isomerization of $CH_3COH^{+\bullet}$ and $CH_3CHO^{+\bullet}$ with water under Fourier transform ion cyclotron resonance (FT-ICR) conditions and observed that the bimolecular reaction proceeded via a catalyzed 1,2 H-transfer. The potential energy surface was also calculated by them, and it showed that the reactions for H_2O loss and for $^{\bullet}CH_3$ loss shared the same transition state (TS1/4), an unusual situation for a reaction pathway. As will be described below, our calculations at the B3-LYP/6-31+G(d) and G3 levels of theory showed that the above two reactions take place via different pathways; that is, a distinguishable transition state leads to each product corresponding to the loss of H_2O or $^{\bullet}CH_3$. In addition to the

† Part of the "Chava Lifshitz Memorial Issue".

* Corresponding author. Phone: (+1) 613 562 5118. Fax: (+1) 613 562 5170. E-mail: jholmes@science.uottawa.ca.

10.1021/jp057108r CCC: $33.50
Published on Web 04/14/2006

isomerization between water-solvated $CH_3COH^{+\bullet}$ and $CH_3CHO^{+\bullet}$ that was discussed in Nedev et al.'s paper,[18] we have also investigated the potential energy surface that includes the interconversion paths involving acetaldehyde's enol ion, $CH_2CHOH^{+\bullet}$, and the above two species.

The acetaldehyde/H_2O system was first studied by Cao et al.[19] in this laboratory, and a new $CH_6O^{+\bullet}$ ion was found to be produced by the loss of CO from the metastable $[CH_3CHO/H_2O]^{+\bullet}$ ion. However, a detailed mechanism for this and other reactions was not provided. In the present work, we have explored in greater detail the isomerization and decomposition chemistry of water-solvated acetaldehyde ions and other isomers including the carbene and vinyl alcohol ions. We also describe the structures of new fragment ions produced by H_2O and $^{\bullet}CH_3$ loss, and complete potential energy surfaces have been established to delineate the reaction mechanism.

Experimental Approach

The experiments were performed on a modified VG ZAB research mass spectrometer[20] (VG Analytical, Manchester, U.K.), which incorporates a magnetic analyzer followed by two electrostatic analyzers (i.e., BEE geometry). Metastable ion (MI) and collision-induced dissociation (CID) mass spectra of selected proton-bound pairs were acquired in the usual manner in the mass spectrometer.[21] The desired ion−molecule complex was produced by CID of the appropriate proton-bound pair in the second field-free region (2FFR) of the instrument. MI and CID dissociations of the ion−molecule complex were observed in the third field-free region (3FFR). The ion accelerating voltage of the proton-bound pairs was 8 kV. In the 2FFR and 3FFR, helium was used as the collision gas. All spectra were recorded with the ZABCAT program developed by Mommers Technologies (Ottawa, Ontario).[20]

The proton-bound dimer of acetaldehyde and ethanol was generated by admitting the mixed reagents into a high pressure ion source via the liquid septum inlet. The pressure in this high pressure source is approximately 1 order of magnitude higher than that achievable in a standard lower pressure source. The pressure in the ion source chamber, read with an ionization gauge located above the ion source diffusion pump, was $\sim 8 \times 10^{-5}$ mbar, indicating an in-source pressure of $\sim$0.3 mbar.[22] The proton-bound dimer $CH_3CHO\cdots H^+\cdots O(H)CH_2CH_3$ (*m*/*z* 91) was mass-selected by the magnet and dissociated by collision in the second field-free region. The fragment ion $[CH_3CHO/HO(H)]^{+\bullet}$ (*m*/*z* 62) resulting from the loss of $CH_3CH_2^{\bullet}$ from the precursor ion (*m*/*z* 91) was transmitted into the third field-free region in order to observe its MI and CID characteristics.

The molecules CH_3CHO and CH_3CH_2OH and the isotopically labeled compounds CD_3CHO and CD_3CDO were used to generate various isotopomeric ion−molecule pairs. The unlabeled chemicals were purchased from Aldrich, and all of the labeled samples, of 99.5−99.9% isotopic purity, were obtained from CDN Isotopes (Montreal, QC, Canada) and were used without further purification.

Theoretical Approach

Standard ab initio molecular orbital calculations[23] were performed using the Gaussian 98 programs[24] to investigate the potential energy surface. Optimized geometries and the energies of all minima and transition states were calculated using Becke three-parameter exchange[25] with the functional of Lee−Yang−Parr correlation[26] (B3-LYP) and the 6-31+G(d) basis set. Vibrational frequency analysis was performed to confirm that the equilibrium and transition state structures were obtained. Intrinsic reaction coordinate (IRC) calculations have been used to follow the reaction paths from all transition states in order to identify intermediates. IRCs were also used to test whether a transition state is the correct structure that connects two minimum wells. G3 single-point energy calculations were carried out on the optimized B3-LYP/6-31+G(d) geometries of all the stable and transition states. G3 theory approximates[27] the energy of a species at the QCISD(T)/G3large level of theory by a series of additive corrections to a base MP4/6-31+G(d) energy. The G3large (or GTlarge) basis set is a modified version of the standard 6-311+G(3df,2p) basis set in which more polarization functions are added to first-row elements (3d2f), fewer on second-row elements (2df), and core polarization functions are incorporated. A scaling factor of 0.96[28] was used in G3 calculations for the zero-point vibrational energies (ZPE) obtained from B3-LYP/6-31+G(d). MP2(full)/G3large calculation was used to take into account core-correlation contributions, and empirical higher level correction (HLC) was employed to correct residual basis-set errors. The heats of formation of new products, those resulting from the losses of H_2O and $^{\bullet}CH_3$, were obtained by converting their G3 total energies into enthalpies of the ions, based on the atomization method reported by Nicolaides et al.[29] The 298 K heats of formation were evaluated with the aid of standard thermodynamic formulas in conjunction with the B3-LYP/6-31+G(d) frequencies and experimental thermocorrections for the elements.[30] The binding energies of the electrostatically bound species were calculated from the difference in energy between the intact cluster and the dissociation products.

Results and Discussion

Dissociation Reactions of the $[CH_3CHO/H_2O]^{+\bullet}$ Ion−Molecule Complex. The MI mass spectrum of the proton-bound dimer $CH_3CHO\cdots H^+\cdots O(H)CH_2CH_3$ (*m*/*z* 91) shows two peaks, that is, protonated ethanol (*m*/*z* 47) and protonated acetaldehyde (*m*/*z* 45) (PA$[CH_3CHO]$ = 768.5 kJ/mol,[17] PA$[CH_3CH_2OH]$ = 777 kJ/mol).[17] These are the only MI processes, showing that no rearrangement of the proton-bound dimer occurs at internal energies up to those for MI dissociations. This proton-bound dimer readily lost a $CH_3CH_2^{\bullet}$ radical by collisional excitation, showing a signal at *m*/*z* 62, the reaction shown in eq 2. The *m*/*z* 62 peak intensified with additional collision gas, and when the main beam had been reduced by $\sim$20%, it was intense enough to be transmitted (by the electrostatic sector) into the third free-field region in order for its dissociation characteristics to be studied.

$$\underset{m/z\ 91}{CH_3CHO\cdots H^+\cdots O(H)CH_2CH_3} \rightarrow [CH_3CHO/HOH]^{+\bullet} + CH_3CH_2^{\bullet}\ (\text{CID}) \quad (2)$$
$$m/z\ 62\ (\text{ion } \mathbf{1})$$

The MI mass spectrum of ion **1**, Figure 1A, shows three competing dissociation processes: the losses of $^{\bullet}CH_3$ (*m*/*z* 47, 44%), H_2O (*m*/*z* 44, 100%), and CO (*m*/*z* 34, 56%). The observation that a metastable ion peak is insensitive to collision gas signifies that the mass-selected ion has undergone a rearrangement to an isomeric species over an energy barrier close to the lowest energy fragmentation for that ion.[31] In cases where this energy barrier is lower or nonexistent, the collision sensitivity of the peak is correspondingly greater. If the MI peak arises from a simple bond cleavage in the mass-selected ion, the collision sensitivity is great and often produces the base

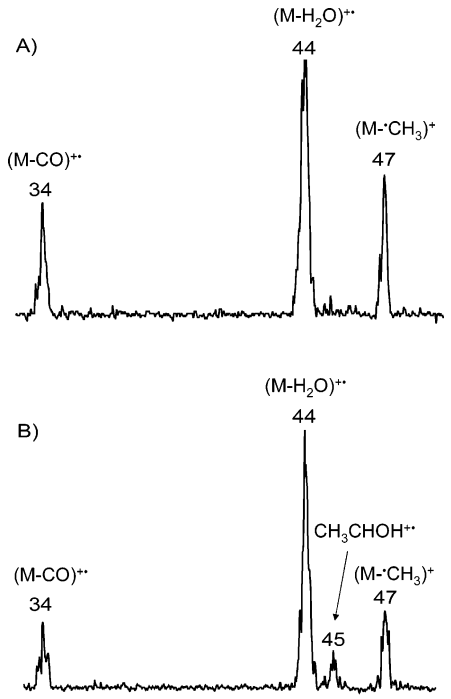

Figure 1. (A) MI mass spectrum of $[CH_3CHO/H_2O]^{+\bullet}$, ion **1**. (B) CID mass spectrum of $[CH_3CHO/H_2O]^{+\bullet}$, ion **1**.

peak in a CID mass spectrum.[31] In the CID mass spectrum of ion **1**, Figure 1B, the peak at *m*/*z* 45, CH_3CHOH^+, intensifies, from having been barely visible in the MI mass spectrum. The formation of CH_3CHOH^+, *m*/*z* 45, being a simple bond cleavage in ion **1**, is thus collision sensitive. This indicates that ion **1** has kept the proton-bridged form of the precursor proton-bound pair, *m*/*z* 91, and so its structure is better represented as $[CH_3C(H)OH^+\cdots{}^{\bullet}O(H)]$. The proton is more strongly attached to acetaldehyde because the PA of CH_3CHO at O, 768.5 kJ/mol,[32] is significantly higher than that of $^{\bullet}OH$, 593 kJ/mol.[17] However, note that the peak at *m*/*z* 44 is also slightly *sensitive* to the collision gas, indicating that at least some of ion **1** can be represented as $CH_3CHO^{+\bullet}/H_2O$, an acetaldehyde ion electrostatically bound to a water molecule, in keeping with acetaldehyde having a lower ionization energy (IE) than water, (IE[CH_3CHO] = 10.2 eV, IE[H_2O] = 12.6 eV).[33]

What is the product ion resulting from H_2O loss from the $[CH_3CHO/H_2O]^{+\bullet}$ complex, $CH_3CHO^{+\bullet}$, $CH_2CHOH^{+\bullet}$, $CH_3COH^{+\bullet}$, or a mixture of these ions? Isotopic labeling experiments indicate that vinyl alcohol ions (*m*/*z* 44) are produced, but some keto (acetaldehyde) ions remain. The MI mass spectra of three isotopic labeled samples, $[CH_3CHO/D_2O]^{+\bullet}$ (*m*/*z* 64, ion **1**-d_2), $[CD_3CHO/H_2O]^{+\bullet}$ (*m*/*z* 65, ion **1**-d_3), and $[CD_3CDO/H_2O]^{+\bullet}$ (*m*/*z* 66, ion **1**-d_4), provided consistent results showing that the enol ion was produced (Figure 2). The fully deuterated acetaldehyde was used to form $[CD_3CDO/H_2O]^{+\bullet}$. Its MI mass spectrum is shown in Figure 2A, in which the second most intense peak is due to the loss of −HDO rather than the direct loss of H_2O. This *m*/*z* 47 ion produced by ion **1**-d_4 is proposed to have the enol structure $CD_2CDOH^{+\bullet}$. In the MI mass spectrum of $[CD_3CHO/D_2O]^{+\bullet}$, Figure 2B, the enol ion appears at *m*/*z* 46, $CD_2CHOH^{+\bullet}$. Note that the loss of H_2O or a methyl radical ($-{}^{\bullet}CD_3$) from ion **1**-d_4 and ion **1**-d_3 produces only an (M − 18) ion. Figure 2C shows that the dissociation of metastable $[CH_3CHO/D_2O]^{+\bullet}$ ions produces $CH_3CHO^{+\bullet}$ (*m*/*z* 44) and $CH_2CHOD^{+\bullet}$ (*m*/*z* 45) in a ratio of approximately 1.9:1. The above three experiments show that the mechanism for generating the enol (vinyl alcohol ion) involves moving the

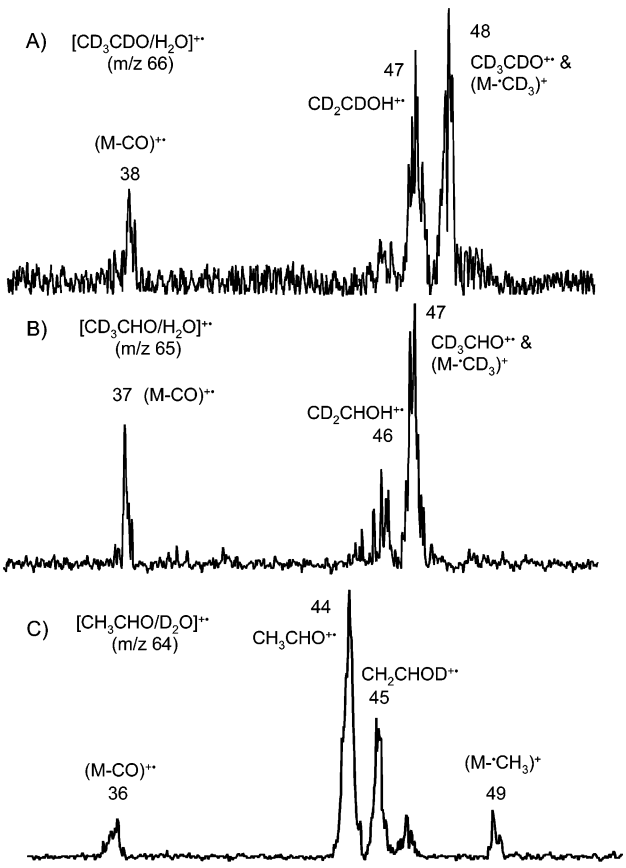

Figure 2. (A) MI mass spectrum of $[CD_3CDO/H_2O]^{+\bullet}$ (*m*/*z* 66, ion **1**-d_4). (B) MI mass spectrum of $[CD_3CHO/H_2O]^{+\bullet}$ (*m*/*z* 65, ion **1**-d_3). (C) MI mass spectrum of $[CH_3CHO/D_2O]^{+\bullet}$ (*m*/*z* 64, ion **1**-d_2).

proton to the carbonyl oxygen and shifting a methyl H to the $^{\bullet}OH$ group. The reaction path and transition state of such a rearrangement is shown on the potential energy surface (PES) (Figure 3).

The dissociation channel that leads to $CH_2CHOH^{+\bullet}$ is enthalpically more favorable than that for producing other isomers of $C_2H_4O^{+\bullet}$. The dissociation limit for the generation of $CH_2CHOH^{+\bullet}$ is 529 kJ/mol (from $\Delta_f H[{}^{\bullet}CH_2CHOH^+] = 771$ kJ/mol,[34] $\Delta_f H[H_2O] = -242$ kJ/mol[34]). This is lower than the dissociation limit, 579 kJ/mol, for the formation of the acetaldehyde ion (from $\Delta_f H[CH_3CHO^{+\bullet}] = 821$ kJ/mol[34]). Although the dissociation leading to $CH_2CHOH^{+\bullet}$ is lower in energy, whether the $CH_3CHO^{+\bullet}$ isomerized to $CH_2CHOH^{+\bullet}$ within the complex $[CH_3CHO/H_2O]^{+\bullet}$ depends on whether there is a barrier for the tautomerization. The reaction path is shown in the potential energy surface, Figures 4 and 5 (see also the discussion below). In addition, the threshold energy (623 kJ/mol) for dissociation to the carbene ion ($CH_3COH^{+\bullet}$) and water is much higher (from $\Delta_f H[(CH_3COH^{+\bullet}] = 865$ kJ/mol[34]), and is energetically the least favorable process, and thus, this dissociation channel can be ruled out.

The $(M - 28)^{+\bullet}$ peak is common to the mass spectra of all the deuterated samples, and there are no $(M - 29 \text{ or } 30)^{+\bullet}$ peaks (see Figure 2). Therefore, this $(M - 28)^{+\bullet}$ ion arises from the loss of a CO molecule and not from C_2H_4, as shown by the labeled samples. This product ion resulting from the loss of CO has been found to be the ion $CH_6O^{+\bullet}$ (a missing member of the remarkable series of ions CH_nO^+, $n = 0-7$). The structure of $CH_6O^{+\bullet}$ was found by computation to be a methyl radical electrostatically bound to protonated water, $[{}^{\bullet}CH_3\cdots H^+OH_2]$, as described by Cao et al.[19]

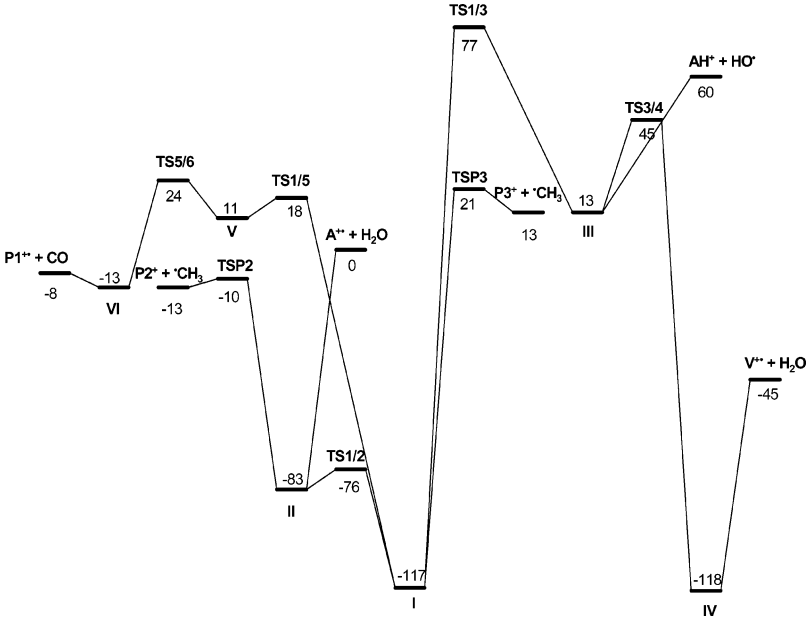

Figure 3. Potential energy surface of $[CH_3CHO/H_2O]^{+\bullet}$ based on calculations at the G3 level of theory. Relative energies are given in kJ/mol.

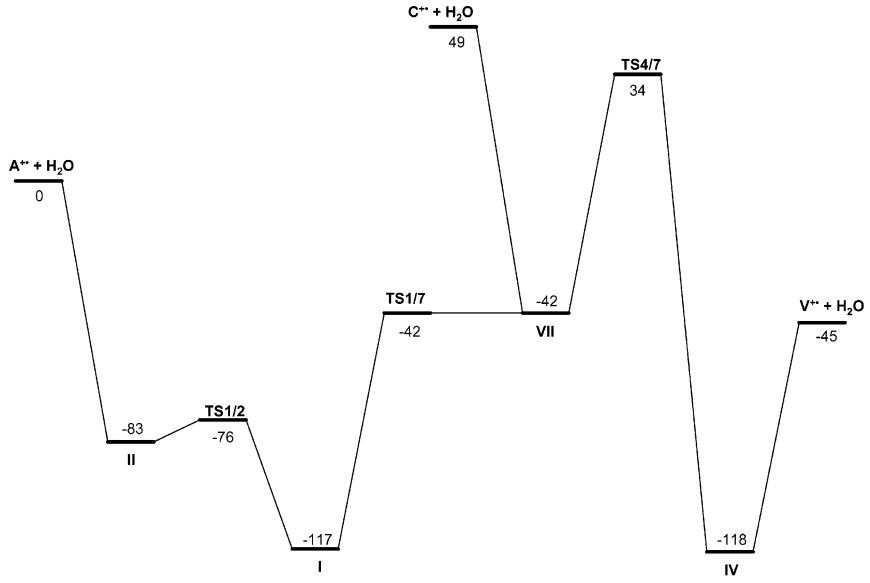

Figure 4. Energy diagram for the water-catalyzed 1,2 H-transfer and PTC isomerizations of the acetaldehyde ion ($CH_3CHO^{+\bullet}$), its carbene (CH_3-$COH^{+\bullet}$), and enol isomers ($CH_2CHOH^{+\bullet}$). The relative energies are calculated at the G3 level of theory and are given in kJ/mol.

The mass spectra of the isotopically labeled samples also show that no isotopic mixing precedes the elimination of a methyl radical and that all the methyl-H atoms of acetaldehyde retain their position prior to the fragmentation. The loss of $^{\bullet}CH_3$ produces a $CH_3O_2^+$ ion which has been characterized by theory and is discussed in the following section.

Computational Analysis of the Chemistry of the $[CH_3CHO/H_2O]^{+\bullet}$ Ion. With the above mass spectrometric experiments as a guide, the theoretical calculations revealed the reaction paths for each dissociation process, that is, the losses of H_2O, $^{\bullet}OH$, $^{\bullet}CH_3$, and CO, respectively. The potential energy profile for the dissociation reactions of the $[C_2H_4O/H_2O]^{+\bullet}$ complex (ion **1**) is shown in Figure 3, on which $A^{+\bullet}$, AH^+, and $V^{+\bullet}$ refer to the acetaldehyde ion, protonated acetaldehyde, and the vinyl alcohol ion, respectively. Eight significant isomers of ion **1** have been found by density functional theory (DFT) calculations at the B3-LYP/6-31+G(d) level to be stable, and their optimized geometries are shown in Figure 6. All relative energies that are indicated on the PESs in this paper refer to G3 results at 0 K and are relative to the sum of the G3 energies of $CH_3CHO^{+\bullet}$ and H_2O.

The acetaldehyde ion/water complex ($[CH_3CHO^{+\bullet}/OH_2]$, stable state II) can readily convert into a more stable structure, I, via a low energy barrier (TS1/2, −76 kJ/mol). A relatively high energy barrier (TS 1/3, 77 kJ/mol), that lies above all of the dissociation limits, prevents the isomerization of isomer I to III, and therefore, it divides the PES (Figure 3) into two parts: the left-hand energy profile incorporates the reaction paths that produce the acetaldehyde ion and the CO and $^{\bullet}CH_3$ loss ions; the right-hand surface involves the generation of the vinyl alcohol ion and protonated acetaldehyde. From the experiments discussed above, ion **1** consists of a mixture of $[CH_3CHO^{+\bullet}/OH_2]$ (complex II) and $[CH_3CHOH^+/^{\bullet}OH]$ (complex III), and the calculations show that complexes II and III cannot freely interconvert at any energy below their dissociation limits.

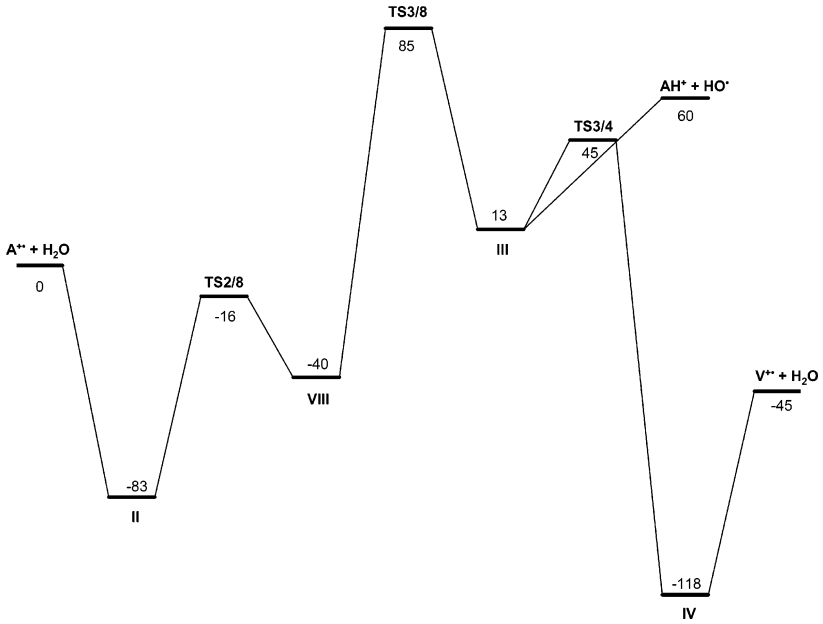

Figure 5. Energy diagram for the H-atom transfer mechanism of keto−enol isomerization of the acetaldehyde ion with water. The relative energies are calculated at the G3 level of theory and are given in kJ/mol.

Therefore, the dissociation reactions of ion **1** involve the chemistry of both II and III.

Complex III rearranges to the vinyl alcohol ion/ water complex, $[CH_2CHOH^{+\bullet}\cdots OH_2]$ (ion IV) via a six-membered transition state, TS3/4. This transition state is ∼15 kJ/mol lower that the dissociation threshold of III (to produce protonated acetaldehyde); ion IV is the global minimum of ion **1**, and thus, the vinyl alcohol ion is produced in the metastable ion time frame (see Figure 1).

The earlier study found the CO loss product to be protonated water electrostatically bound to a methyl radical, $[^{\bullet}CH_3\cdots H^+\text{-}OH_2]$, and the calculated 298 K $\Delta_f H$ was 690 kJ/mol and the binding energy was only 58 kJ/mol based on G3 results.[19] The optimized structure of this ion, $P1^{+\bullet}$, is given in Figure 8. The reaction mechanism has been explored and is shown in the PES (Figure 3). This ion, $P1^{+\bullet}$, is generated from ion **1** by the loss of CO via a "backside displacement" mechanism, as shown in Scheme 1. The first step of this process involves the H_3O^+ back-attacking the acetyl radical through a methyl hydrogen atom to form an intermediate complex, structure V in Figure 6. The second step consists of stretching the C−C bond in the acetyl group and shortening the electrostatic bond between the proton (in H_3O^+) and the methyl radical in the center, followed by the formation of the stable state VI, $[H_2OH^+\cdots{}^{\bullet}CH_3\cdots CO]$. Transition states TS1/5 and TS5/6 correspond to this backside displacement reaction, and their optimized structures are shown in Figure 7.

Methyl loss from ion **1** produces $[C,H_3,O_2]^+$ ions, the most stable isomer of which is protonated formic acid, $\Delta_f H[HC^+\text{-}(OH)_2] = 403$ kJ/mol.[34] However, the transition states involved in this reaction channel leading to protonated formic acid and a methyl radical was calculated to be too high (relative energy is ∼90 kJ/mol) to compete with other dissociation processes in the metastable ion time frame. This transition state involved a 1,3-hydroxyl group migration with a large energy requirement. Possible structures for the $^{\bullet}CH_3$ loss ions have been proposed by calculations to be $[OC\cdots H^+OH_2]$, $P2^+$, and $[CO\cdots H^+OH_2]$, $P3^+$. They are both hydrogen-bridged complex (HBC) ions and represent CO attached to protonated water, similar in type to the CO loss product from ion **1** where the $^{\bullet}CH_3$ radical was the ligand. In $P3^+$, the protonated water and CO are bound via an $O\cdots H^+\cdots O$ bridge and in $P2^+$ via a $C\cdots H^+\cdots O$ bridge. The optimized structures of $P2^+$ and $P3^+$ are shown in Figure 8. The 298 K heats of formation of these two stable $[C,H_3,O_2]^+$ ions were obtained from G3 calculations as $\Delta_f H[OC\cdots H^+OH_2] = 420$ kJ/mol and $\Delta_f H[CO\cdots H^+OH_2] = 448$ kJ/mol. Using these enthalpy values, the binding energies at 298 K have been determined as $[OC\cdots{}^+H_3O] = 66$ kJ/mol and $[CO\cdots{}^+H_3O] = 38$ kJ/mol, respectively, from $\Delta_f H[CO] = -111$ kJ/mol[33] and $\Delta_f H[H_3O^+] = 597$ kJ/mol.[30] Note that these results show that in the above HBC ions the $C\cdots H^+\cdots O$ bond is stronger than the $O\cdots H^+\cdots O$ bond, in contrast with the observation that the latter bond is usually the stronger one in such HBC ions; for example, the ion $CH_3CO^{\bullet}\cdots H^+\cdots OH_2$ is more stable than $CH_3C^{\bullet}(O)\cdots H^+\cdots OH_2$. This is likely due to the greater PA of CO at C (594 kJ/mol)[17] than at O (426 kJ/mol).[17]

It remains to consider whether the isomeric complexes $[OC^{\bullet}\cdots{}^+H_3O]$ and $[CO\cdots{}^+H_3O]$ can freely interconvert. A computational study by Chalk and Radom investigated the catalyzed rearrangement of the formyl cation (HCO^+) to the isoformyl cation (HOC^+) by a wide variety of catalysts.[35] The energy difference between the two $[H,C,O]^+$ isomers is 164 kJ/mol ($\Delta_f H[HCO^+] = 826$ kJ/mol,[34] $\Delta_f H[HOC^+] = 990$ kJ/mol[34]), and there is a significant energy barrier separating them (∼147 kJ/mol above HCO^+). The water-assisted interconversion of the isoformyl and formyl cation was calculated[35] to test whether a water molecule can catalyze the isomerization. However, the optimized ground state IMCs were found to have the configurations $[OC\cdots{}^+H_3O]$ and $[CO\cdots{}^+H_3O]$, rather than $[OCH^+\cdots OH_2]$ and $[COH^+\cdots OH_2]$. Because the PA of H_2O (697 kJ/mol) is much greater than that of CO at either the O or C site, the water molecule readily captures the proton from either HCO^+ or HOC^+. Their G2 calculations showed that the energy difference between $[OC\cdots{}^+H_3O]$ and $[CO\cdots{}^+H_3O]$ is 25 kJ/mol, which is in excellent agreement with the result obtained in this study ($\Delta\Delta_f H = 448$ kJ/mol − 420 kJ/mol = 28 kJ/mol). The barrier for this rearrangement was determined to be 52 kJ/mol.[35] The potential energy diagram (Figure 9) gives the energy for each species and dissociation reaction. The ions $[OC\cdots{}^+H_3O]$ and $[CO\cdots{}^+H_3O]$ reside in separate potential energy wells, and thus,

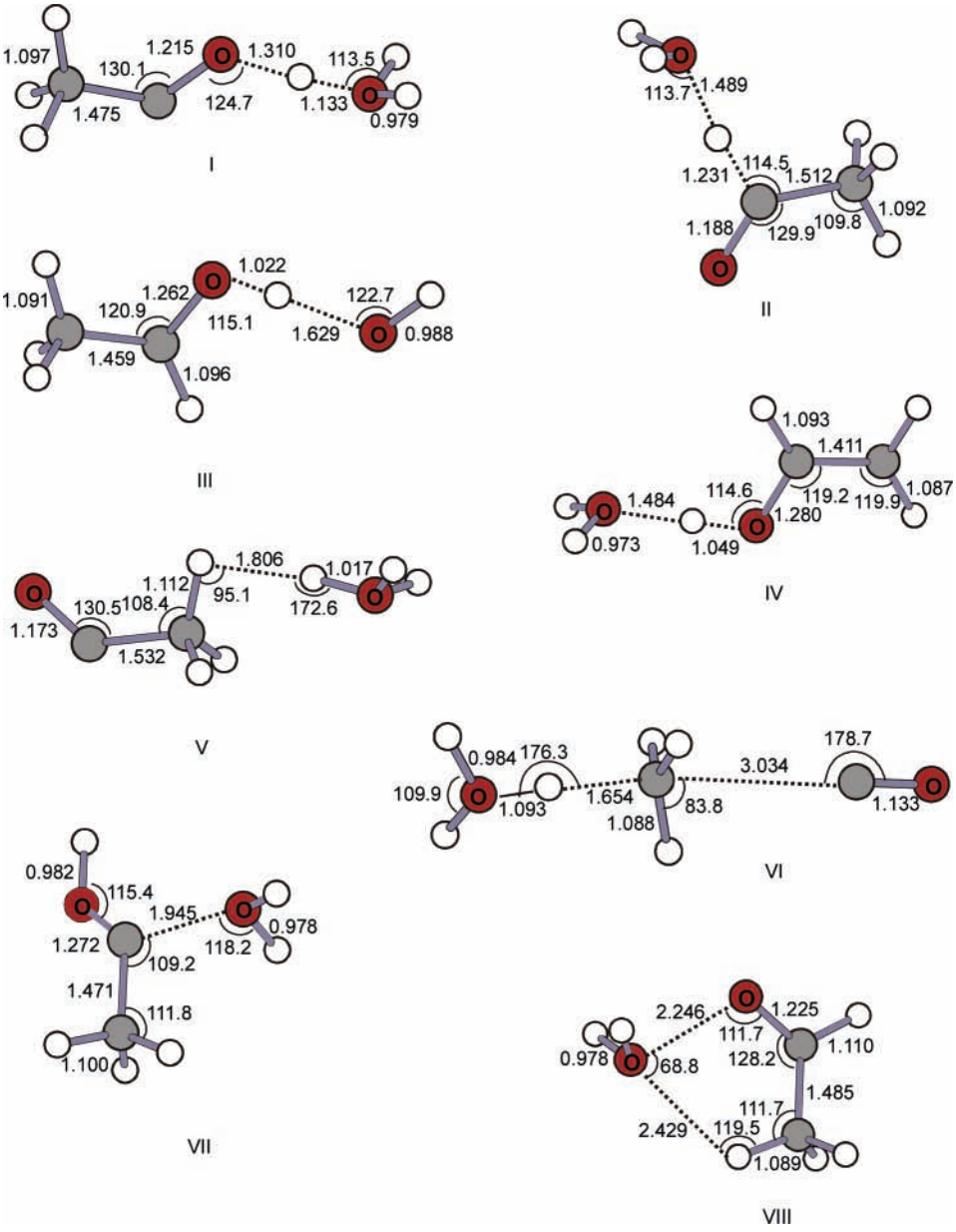

Figure 6. Optimized structures of the intermediate (structure V) and stable states at the B3-LYP/6-31+G(d) level of theory.

they are both stable species. In this study, the two ions are made by different reaction channels and thus both isomers can be obtained in our experiments. The dissociation limit to produce H_3O^+ and CO lies only 9 kJ/mol higher than the transition state, well below that to generate H_2O and OCH^+ or COH^+. Water therefore cannot catalyze the rearrangement from COH^+ to HCO^+, and the dissociation reaction to H_3O^+ and CO is preferred to the proton migration (from the H_2O to CO) to produce the HCO^+ ion.

The $^{\bullet}CH_3$ loss ions are thus produced by the following processes: cleavage of the C−C bond in $[CH_3CHO^{+\bullet}\cdots OH_2]$, complex II, leads to the production of the $[OC\cdots H^+OH_2]$ ion; also, $[CO\cdots H^+OH_2]$ is generated from the C−C bond dissociation of complex I, $[CH_3CO^{\bullet}\cdots H^+OH_2]$. TSP2 and TSP3 are the corresponding transition states for these two dissociations, and their respective configurations are shown in Figure 7.

Mechanisms of Keto−Enol−Carbene Isomerization in $C_2H_4O^{+\bullet}/H_2O$ Ions. For the water-solvated interconversions among the isomers $CH_3CHO^{+\bullet}$ ($A^{+\bullet}$), $CH_3COH^{+\bullet}$ ($C^{+\bullet}$), and $CH_2CHOH^{+\bullet}$ ($V^{+\bullet}$), a proton-transport catalysis mechanism was first considered, because the proton affinity of H_2O (PA = 691 kJ/mol[17]) meets the PA criterion for PTC of $CH_3COH^{+\bullet}$ to $CH_3CHO^{+\bullet}$, lying between the PA value of the C and O sites of the $CH_3CO^{\bullet}$ radical (PA $[CH_3CO^{\bullet}]$ at O = 679 kJ/mol[18] and at C = 694 kJ/mol[18]). For the tautomerization from $CH_3COH^{+\bullet}$ to $CH_2CHOH^{+\bullet}$, the PA of H_2O does not fall in the range of the PA values of the two C atoms in the $CH_2C^{\bullet}OH$ radical. These PA values are estimated to be 882 ± 15 and 788 ± 15 kJ/mol, respectively.[37]

The energy barrier of the rearrangement between isolated $CH_3COH^{+\bullet}$ and $CH_3CHO^{+\bullet}$ was calculated by Bouchoux et al.[38] as 143 kJ/mol which is above the dissociation limit (121 kJ/mol) for the loss of the hydroxyl $H^{\bullet}$ from $CH_3COH^{+\bullet}$. In the present study, the PES (Figure 4) obtained from the G3 calculations shows that a water molecule catalyzes two-step H-shifts in converting $CH_3COH^{+\bullet}$ to $CH_3CHO^{+\bullet}$. Starting from the $[CH_3COH^{+\bullet}/H_2O]$ complex (structure VII), the water molecule abstracts a proton from $CH_3CHO^{+\bullet}$ to form stable state I, $[CH_3CO^{\bullet}/H^+OH_2]$, via a very flat transition state (TS1/7). Next, the water "transports" the H^+ between the C and O site

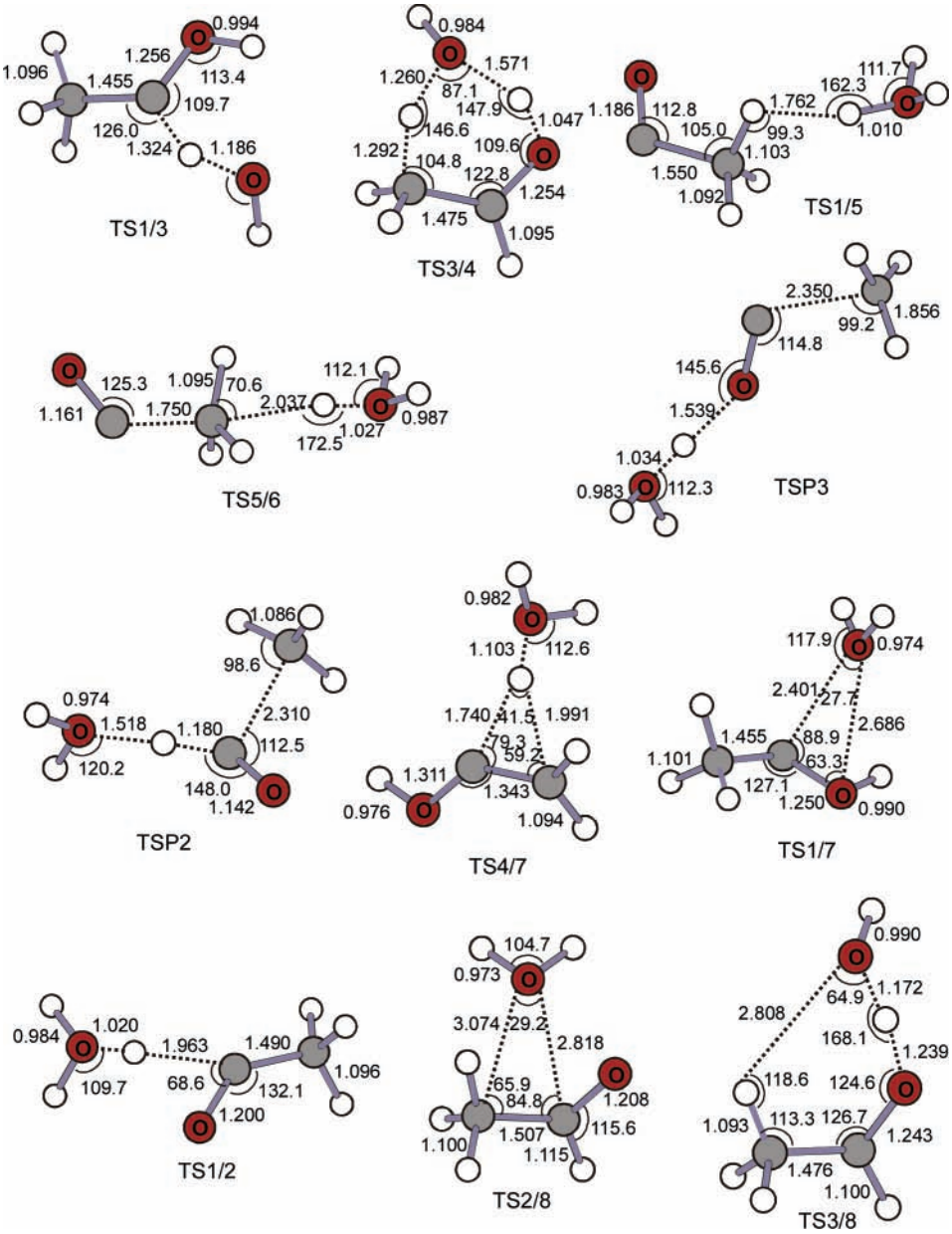

Figure 7. Optimized structures of the transition states at the B3-LYP/6-31+G(d) level of theory.

of the $CH_3CO^{\bullet}$ radical via TS1/2, followed by the production of the ion $[CH_3CHO^{+\bullet}/OH_2]$ (complex II), as shown in eq 3.

$$CH_3COH^{+\bullet} + H_2O \rightarrow [CH_3COH^{+\bullet}/OH_2] \rightarrow [CH_3CO^{\bullet}/H^+OH_2] \rightarrow [CH_3CHO^{+\bullet}/OH_2] \rightarrow CH_3CHO^{+\bullet} + H_2O \quad (3)$$

The energy barriers, TS1/2 (−76 kJ/mol) and TS1/7 (−42 kJ/mol), involved in the above process are lower than the dissociation thresholds to $CH_3COH^{+\bullet} + H_2O$ (49 kJ/mol) or to $CH_3CHO^{+\bullet} + H_2O$ (0 kJ/mol), and thus, water can indeed catalyze the isomerization from $CH_3COH^{+\bullet}$ to $CH_3CHO^{+\bullet}$. However, the reverse reaction in eq 3 does not occur; that is, starting from the $CH_3CHO^{+\bullet} + H_2O$ bimolecular reactant pair cannot produce $CH_3COH^{+\bullet} + H_2O$ because the dissociation energy for the latter is too high and thus only $CH_3CHO^{+\bullet}$ would be the observed product. Therefore, in bimolecular reactions, whether a PTC process can be observed depends on the starting point and on the initial internal energy carried in the bimolecular reactants. For the unimolecular reactions of a given ion's structure, interconversions among all the stable structures that lie below or close above its lowest dissociation limit will be observed in the MI time frame.

We have also observed that a water molecule catalyzes the 1,2 H-shift between C and C sites in a $CH_2^{\bullet}COH$ radical (TS4/7, 34 kJ/mol), resulting in the generation of $CH_2CHOH^{+\bullet}$ and water. The reaction is represented by eq 4.

$$CH_3COH^{+\bullet} + H_2O \rightarrow [CH_3COH^{+\bullet}/OH_2] \rightarrow [CH_2CHOH^{+\bullet}/OH_2] \rightarrow CH_2CHOH^{+\bullet} + H_2O \quad (4)$$

G2 calculations by Bouchoux et al.[38] showed that the energy barrier of the 1,2 H-shift for isolated $CH_3COH^{+\bullet}$ and $CH_2CHOH^{+\bullet}$ ions is 7 kJ/mol lower than the energy barrier to the dissociation of $CH_3COH^{+\bullet}$ to CH_3CO^+ and $H^{\bullet}$. As shown in the PES (Figure 4), the water-assisted transition state (TS4/7) for such a 1,2 H-shift is 15 kJ/mol lower than the dissociation limit of $[CH_3COH^{+\bullet}/H_2O]$ to $CH_3COH^{+\bullet}$ and H_2O. Therefore,

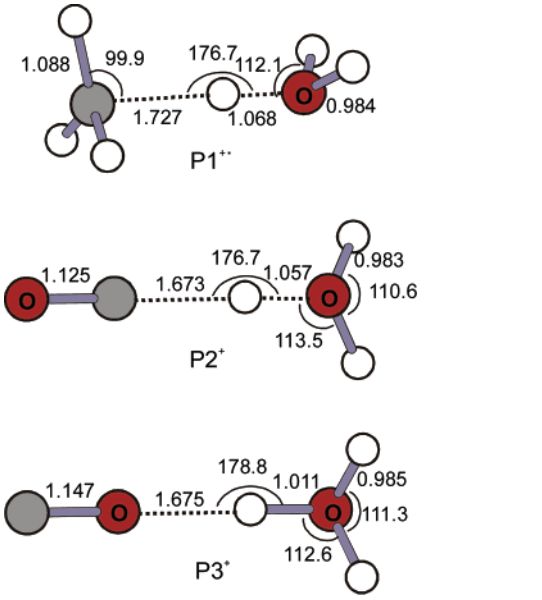

Figure 8. Optimized structures of CO and $^{\bullet}CH_3$ loss products at the B3-LYP/6-31+G(d) level of theory.

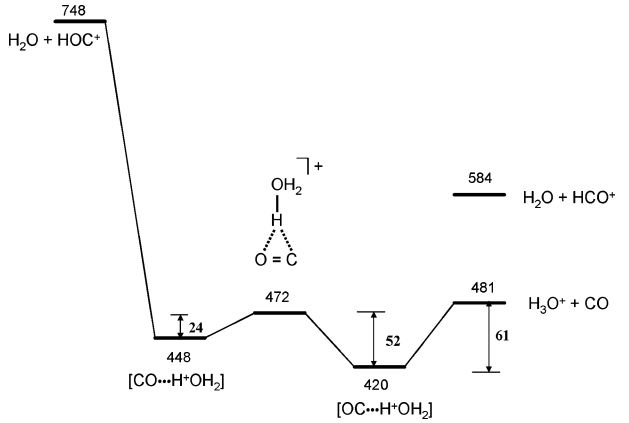

Figure 9. Potential energy diagram for the interconversion between $[OC\cdots{}^{+}H_3O]$ and $[CO\cdots{}^{+}H_3O]$. All energies are given in kJ/mol.

SCHEME 1: "Backside Displacement" Mechanism for the Reaction of the CO Lost from Ion 1

Backside Displacement Mechanism

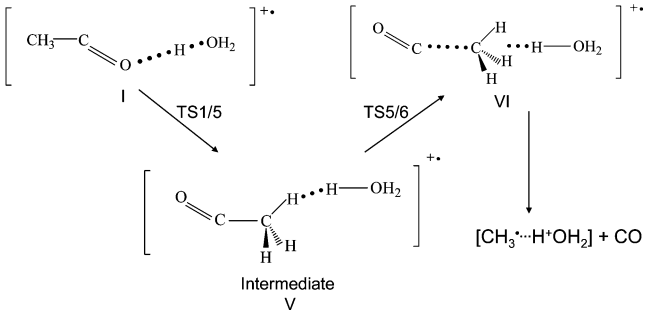

the 1,2 H-shift energy barrier is lowered by the water catalyst by ~8 kJ/mol.

In previous studies,[13,14] we found that the keto−enol isomerization of acetaldehyde and acetone occurred in the presence of a distonic methanol via a H-atom transfer mechanism. Calculations have been performed to examine whether H_2O catalyzed the H-atom transfer process for the rearrangement of $CH_3CHO^{+\bullet}$ to $CH_2CHOH^{+\bullet}$. The reaction path is given by the PES shown in Figure 5. The reaction is shown in eq 5.

$$CH_3CHO^{+\bullet} + H_2O \rightarrow [CH_3CHO^{+\bullet}/OH_2] \rightarrow [CH_3CHOH^{+}/{}^{\bullet}OH] \rightarrow [CH_2CHOH^{+\bullet}/OH_2] \rightarrow CH_2CHOH^{+\bullet} + H_2O \quad (5)$$

A H-atom is transferred from the H_2O to $CH_3CHO^{+\bullet}$ in the $[CH_3CHO^{+\bullet}/H_2O]$ complex (structure VIII) to form the $[CH_3CHOH^{+}/{}^{\bullet}OH]$ complex (Structure III), and this is followed by a methyl-H migration to the $^{\bullet}OH$ group to form $[CH_2CHOH^{+\bullet}/H_2O]$ (complex IV) via TS3/4 (45 kJ/mol). Note that complexes VIII and II (see Figure 6) are isomers of $[CH_3CHO^{+\bullet}/H_2O]$; the latter is more stable and can be reached by the former via TS2/8 (−11 kJ/mol). A high energy barrier (TS3/8, 85 kJ/mol) is involved in the rearrangement from III to VIII and thus makes a H-atom transfer mechanism energetically unfavorable.

Conclusions

The $[CH_3CHO/H_2O]^{+\bullet}$, ion **1**, made by the CID of an appropriate proton-bound dimer, carries sufficient internal energy to undergo metastable ion dissociations in the 3FFR of the mass spectrometer. The product ion from the loss of H_2O has been shown to have the $CH_2CHOH^{+\bullet}$ structure by isotopic labeling experiments, indicating that rearrangement occurs prior to the dissociation. Theoretical calculations were used to analyze the rearrangement and dissociation reactions of this complex ion and were found to involve no less than eight stable isomers of $[CH_3CHO/H_2O]^{+\bullet}$. The interconversions among these stable isomers can be observed so long as transition state energy barriers lie below the dissociation limit of the initial ion structure. These methods provide us with insight into the chemistry of these ion−molecule complexes, rather than only to focus on the production of keto, enol, or carbene ions. As the PA rule predicts, water is able to catalyze the proton transfer processes for the isomerization of $CH_3COH^{+\bullet}$ to $CH_3CHO^{+\bullet}$. The rearrangement of $CH_3COH^{+\bullet}$ to $CH_2CHOH^{+\bullet}$ involves a water-catalyzed 1,2 H-shift mechanism. $CH_3CHO^{+\bullet}$ cannot be enolized by water to $CH_2CHOH^{+\bullet}$ via either PTC or a H-atom transfer mechanism.

The hydrogen-bridged water complexes ($[X\cdots H^{+}\cdots OH_2]$ shown in detail in Figure 8) are the major products of the losses of CO and $^{\bullet}CH_3$. An unexpected CO loss produced the $[^{\bullet}CH_3\cdot\cdot\cdot H_3O^{+}]$ ion via a backside displacement mechanism. The products resulting from $^{\bullet}CH_3$ loss have been shown by computations to be $[OC\cdots H_3O^{+}]$ and $[CO\cdots H_3O^{+}]$, and their 298 K enthalpies are $\Delta_f H[OC\cdots H_3O^{+}] = 420$ kJ/mol and $\Delta_f H[CO\cdots H_3O^{+}] = 448$ kJ/mol (G3 results).

Acknowledgment. The authors acknowledge the Natural Sciences and Engineering Research Council of Canada for continuing financial support. Special thanks go to Dr. P. M. Mayer for his assistance with the computations. This paper is dedicated to the memory of Chava Lifshitz, a fine scientist and a good friend.

Supporting Information Available: Archive entries for all stable states, transition states, and products on the potential energy surfaces. This material is available free of charge via the Internet at http://pubs.acs.org.

References and Notes

(1) McAdoo, D. J. *Mass Spectrom. Rev.* **1988**, *7*, 363−393.
(2) Hammerum, S. *J. Chem. Soc., Chem. Commun.* **1988**, *13*, 858−859.
(3) Morton, T. H. *Tetrahedron* **1982**, *38*, 3195−3243.
(4) Morton, T. H. *J. Am. Chem. Soc.* **1980**, *102*, 1596−1602.

(5) Longevialle, P.; Botter, R. *J. Chem. Soc., Chem. Commun.* **1980**, *17*, 823−825.
(6) Gauld, J. W.; Audier, H.; Fossey, J.; Radom, L. *J. Am. Chem. Soc.* **1996**, *118*, 6299−6300.
(7) Gauld, J. W.; Radom, L. *J. Am. Chem. Soc.* **1997**, *119*, 9831−9839.
(8) Bohme, D. K. *Int. J. Mass Spectrom. Ion Processes* **1992**, *115*, 95−110 and references therein.
(9) Chalk, A. J.; Radom, L. *J. Am. Chem. Soc.* **1997**, *119*, 7573−7578.
(10) Chalk, A. J.; Radom, L. *J. Am. Chem. Soc.* **1999**, *121*, 1574−1581.
(11) Fridgen, T. D.; Parnis, J. M. *Int. J. Mass Spectrom.* **1999**, *190*/*191*, 181−194.
(12) Tu, Y.-P.; Holmes, J. L. *J. Am. Chem. Soc.* **2000**, *122*, 3695−3700.
(13) Wang, X.; Holmes, J. L. *Int. J. Mass Spectrom.* **2005**, *242*, 75−85.
(14) Wang, X.; Holmes, J. L. *Can. J. Chem.* **2005**, *83*, 1−10.
(15) Mourgues, P.; Audier, H. E.; Leblanc, D.; Hammerum, S. *Org. Mass Spectrom.* **1993**, *27*, 1098−1100.
(16) Audier, H. E.; Leblanc, D.; Mourgues, P.; McMahon, T. B. *J. Chem. Soc., Chem. Commun.* **1994**, *20*, 2329−2330.
(17) Hunter, E. P. L.; Lias, S. G. *J. Phys. Chem. Ref. Data* **1998**, *27*, 413−656.
(18) Nedev, H.; Rest, G. v. d.; Mourgues, P.; Audier, H. E. *Eur. J. Mass Spectrom.* **2003**, *9*, 319−326.
(19) Cao, J.; Sun, W.; Holmes, J. L. *Int. J. Mass Spectrom.* **2002**, *217*, 179−184.
(20) Holmes, J. L.; Mayer, P. M. *J. Phys. Chem.* **1995**, *99*, 1366−1370.
(21) Busch, K. L.; Glish, G. L.; McLuckey, S. A. *Mass Spectrometry/Mass Spectrometry Techniques and Applications of Tandem Mass Spectrometry*; VCH Publishers: New York, 1988.
(22) Rennie, E.; Mayer, P. M. *J. Chem. Phys.* **2004**, *120*, 10561−10578.
(23) Hehre, W. J.; Radom, L.; Schleyer, P. v. R.; Pople, J. A. *Ab Initio Molecular Orbital Theory*; John Wiley & Sons: New York, 1986.
(24) Frisch, M. J.; Trucks, G. W.; Schlegel, H. B.; Scuseria, G. E.; Robb, M. A.; Cheeseman, J. R.; Zakrzewski, V. G.; Montgomery, J. A.; Stratmann, R. E.; Burant, J. C.; Dapprich, S.; Millam, J. M.; Daniels, A. D.; Kudin, K. N.; Strain, M. C.; Farkas, O.; Tomasi, J.; Barone, V.; Cossi, M.; Cammi, R.; Mennucci, B.; Pomelli, C.; Adamo, C.; Clifford, S.; Ochterski, J.; Petersson, G. A.; Ayala, P. Y.; Cui, Q.; Morokuma, K.; Malick, D. K.; Rabuck, A. D.; Raghavachari, K.; Foresman, J. B.; Cioslowski, J.; Ortiz, J. V.; Stefanov, B. B.; Liu, G.; Al-Laham, A.; Peng, C. Y.; Nanayakkara, A.; Gonzalez, C.; Challacombe, M.; Gill, P. M. W.; Johnson, B.; Chen, W.; Wong, W. W.; Andres, J. L.; Gonzalez, C.; Head-Gordon, M.; Replogle, E. S.; Pople, J. A. *Gaussian 98*, revision A.7; Gaussian, Inc.: Pittsburgh, PA, 1998.
(25) Becke, A. D. *Phys. Rev. A* **1988**, *38*, 3098−3100.
(26) Lee, C.; Yang, W.; Parr, R. G. *Phys. Rev. B* **1988**, *37*, 785−789.
(27) Curtiss, L. A.; Raghavachari, K.; Redfern, P. C.; Rassolov, V.; Pople, J. A. *J. Chem. Phys.* **1998**, *109*, 7764.
(28) Baboul, A. G.; Curtiss, L. A.; Redfern, P. C.; Raghavachari, K. *J. Chem. Phys.* **1999**, *110*, 7650−7657.
(29) Nicolaides, A.; Rauk, A.; Gluckhovtsev, M. N.; Radom, L. *J. Phys. Chem.* **1996**, *100*, 17460−17464.
(30) Scott, A. P.; Radom, L. *J. Phys. Chem.* **1996**, *100*, 16502−16513.
(31) Holmes, J. L. In *The Encyclopedia of Mass Spectrometry*; Armentrout, P. B., Ed.; Elsevier: Amsterdam, The Netherlands, 2003; Vol. 1, pp 91−98.
(32) van der Rest, G.; Nedev, H.; Chamot-Rooke, J.; Mourgues, P.; McMahon, T. B.; Audier, H. E. *Int. J. Mass Spectrom.* **2000**, *202*, 161−174.
(33) *NIST Chemistry Webbook; NIST Standard Reference Database Number*; National Institute of Standards and Technology: Gaithersburg, MD, 1998.
(34) Lias, S. G.; Bartmess, J. E.; Liebman, J. G.; Holmes, J. L.; Levin, R. D.; Mallard, W. G. *J. Phys. Chem. Ref. Data* **1988**, *17* (Suppl. 1), 1−861.
(35) Chalk, A. J.; Radom, L. *J. Am. Chem. Soc.* **1997**, *119*, 7573−7578.
(36) Luo, Y.-R. *Handbook of Bond Dissociation Energies in Organic Compounds*; CRC Press: Boca Raton, FL, 2003.
(37) The effect of −OH substitution at an olefinic carbon or at a hydrocarbon radical site can readily be estimated from available data in refs 33 and 36, and it lies in the range -177 ± 12 kJ/mol. $\Delta_f H[CH_2C^{\bullet}OH]$ can thus be given a value of $(300 \pm 3 - 177 \pm 12 = 123 \pm 15)$ kJ/mol. Even with this uncertainty, the PAs of this radical at methylene (788 ± 15 kJ/mol) and at the radical site (882 ± 15 kJ/mol) are both high above that of H_2O, PA = 691 kJ/mol.
(38) Bertrand, W.; Bouchoux, G. *Rapid Commun. Mass Spectrom.* **1998**, *22*, 1697−1700.